ELSEVIER

Journal of Molecular Structure: THEOCHEM 732 (2005) 211–218

THEO CHEM

www.elsevier.com/locate/theochem

Theoretical and experimental study of the inelastic neutron scattering spectra of β-5-Nitro-2,4-dihydro-3H-1,2,4-triazol-3-one

Jennifer A. Ciezak*, S.F. Trevino

Weapons and Materials Research Directorate, U.S. Army Research Laboratory, Aberdeen Proving Ground, MD 21005, USA

Received 27 June 2005; revised 15 July 2005; accepted 15 July 2005

Abstract

The inelastic neutron scattering (INS) spectra of β-5-Nitro-2,4-dihydro-3H-1,2,4-triazol-3-one (β-NTO) are presented to 1400 cm^{-1}. The β-NTO vibrational frequencies observed differ considerably from the α-NTO vibrational frequencies and normal mode frequency calculations for the isolated molecule. The INS spectrum contains detail unobserved in the previous IR studies, including combinations and overtones of the phonon and internal modes of β-NTO. The INS spectra are compared with periodic DFT calculations to show that the periodic DFT results correctly predict the solid-state molecular vibrational frequencies.

Keywords: β-NTO; Inelastic neutron scattering; NTO; 5-Nitro-2,4-dihydro-3H-1,2,4-triazol-3-one

1. Introduction

5-Nitro-2,4-dihydro-3H-1,2,4-triazol-3-one (NTO) was first characterized as an insensitive energetic material in 1988 [1]. The insensitivity of NTO to heat, friction, and impact makes it suitable for a wide variety of applications, such as explosive formulations, plastic-bonded explosives, and as a sodium azide replacement in automobile air bag systems [2]. The insensitivity of NTO has been attributed to the broad range of decomposition mechanisms, such as nitrogen–hydrogen bond cleavage, auto-catalysis, and NO_2 elimination with the formation of amide fragments [3]. The exact decomposition mechanism has yet to be elucidated, but a wide range of activation energies suggests that thermal decomposition is highly dependent on environmental conditions [4]. Hydrogen bonding has also been proposed play a key role in the insensitivity of other energetic materials, such as TATB [5] and ANPZ [6]. Evidence of hydrogen bonding in the solid-state of NTO has been observed in both X-ray diffraction [7] and spectroscopic studies [4].

Crystals of NTO have been examined in some detail. Two polymorphic phases are known to exist. The α-polymorph is the most stable, but an accurate crystal structure has yet to be determined because it undergoes a significant degree of twinning [2].

β-NTO forms a monoclinic ($P2_1/c$) unit cell with each molecule linked by four hydrogen bonds, which follow a helical 2_1-screw axis. The crystal structure of β-NTO at 100 K is presented in Fig. 1. X-ray diffraction investigations into the variable temperature crystal structure were performed in the range of 100–298 K [7]. Both thermal expansion, observed in the plane perpendicular to the molecules, and thermal contraction, noted along the hydrogen bond axis, was found, which indicates the anharmonic character of β-NTO [7].

An intermolecular packing potential was developed to describe the β-NTO structure within the approximation of the rigid molecule [8]. The potential was based on the earlier derivation of intramolecular force fields of β-NTO in both the gas and solid-state phases. These force fields were partially constructed from experimental and calculated vibrational frequencies. A close correlation was observed between the experimental vibrational frequencies and a partial IR spectrum of α-NTO published by Lee and Gilardi [9]. The positions of the vibrational mode frequencies were found to vary considerably between the infrared spectra of pure NTO films and NTO molecules isolated in an argon

* Corresponding author. Address: 100 Bureau Dr. MS 8562 Gaithersburg, MD 20899, USA. Tel.: +1 301 975 6082; fax: +1 301 921 9847.
E-mail address: jciezak@arl.army.mil (J.A. Ciezak).

0166-1280/$ - see front matter © 2005 Published by Elsevier B.V.
doi:10.1016/j.theochem.2005.07.022

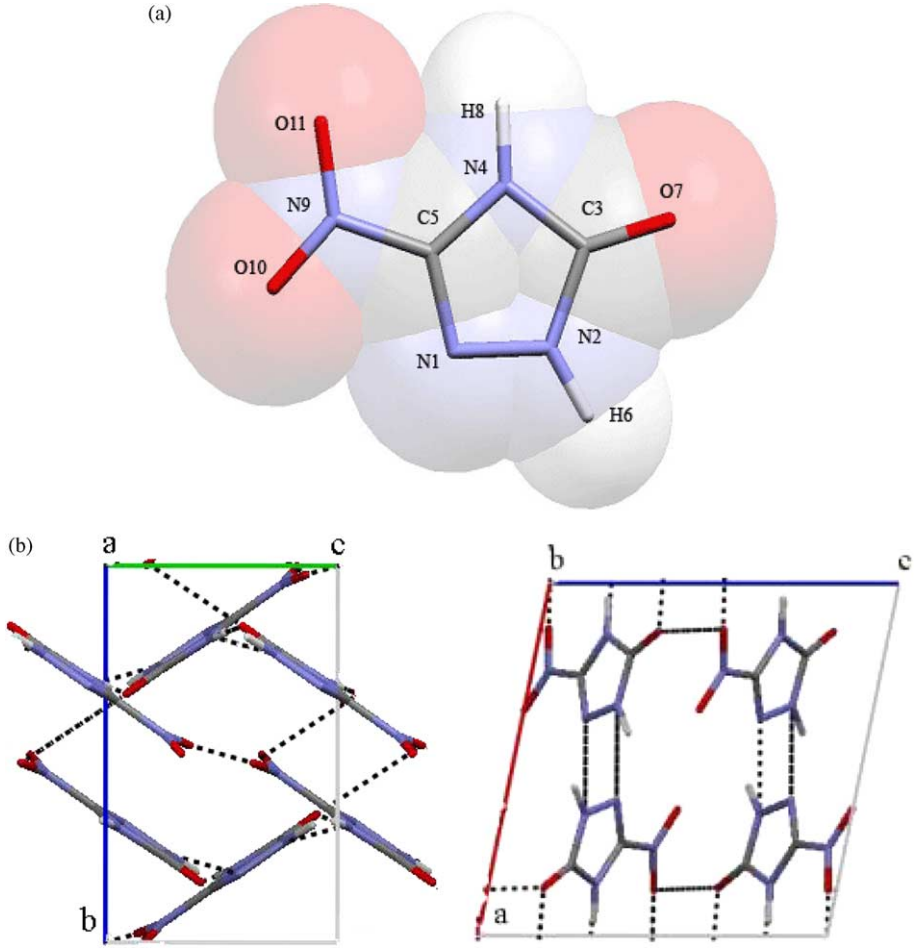

Fig. 1. (a) The numbering scheme and molecular structure of a generic NTO molecule. (b) The crystal structure of β-NTO shown, at left, along the *a* crystallographic axis and, at right, along the *b* crystallographic axis. Dashed lines indicate hydrogen bonds.

matrix, indicating the considerable hydrogen-bonding interaction in the solid-state [8]. In this paper, we bring to evidence that the vibrational frequencies of the two polymorphs of NTO differ considerably and that the vibrational frequencies of β-NTO can be adequately described with solid-state density functional theory (DFT).

Vibrational spectroscopy has been extensively used to investigate the structural details and dynamical interactions in energetic materials [4,5,9–24]. Dlott's theory of 'vibrational up-pumping' through 'doorway' modes [21] has generated interest in the low-frequency spectral region below 700 cm^{-1}. Doorway modes are vibrations that arise because of weak anharmonic coupling between the phonons and intermolecular modes [21–23]. Previous work has indicated that energy transfer into vibrational modes below 700 cm^{-1} may be rate determining [24]. Nevertheless, vibrational information in this spectral region is often incomplete due to instrumental limitations or optical based selection rules. In these cases, inelastic neutron scattering (INS) spectroscopy is an attractive alternative to conventional vibrational spectroscopic methods. The INS intensity of all lattice and molecular vibrations is proportional to the displacements of the hydrogen atoms for a normal mode. The INS spectrum can be directly correlated to computational methods through calculation of the rms displacements of the mass-weighted normal mode hydrogen eigenvectors. This combined INS/DFT approach has been developed extensively over the last decade and has generated considerable success in interpreting vibrational spectra [14,15,25–32]. INS is limited, in a sense, by the resolution of the spectrometers, but this is offset by the wealth of information available in the accessible spectral region [32].

2. Method

2.1. Experimental methods

The β-NTO experiment was performed at the NIST Center for Neutron Research [33] using the Filter Analyzer Neutron Spectrometer (FANS) and the Fermi-Chopper time-of-flight (TOF) instrument. Detailed descriptions of the FANS instrument [34,35] and the TOF instrument [36]

are available. Polycrystalline samples of ca. 1 g were held at 15 K for these experiments. β-NTO was obtained from Picitinny Arsenal and used without further purification. The sample was found to be slightly hygroscopic and attempts were made to dry the sample in a vacuum oven. The INS spectra of β-NTO were normalized for the background contribution by using the DAVE program [37].

2.2. Computational methods

The β-NTO crystal structure used for the solid-state DFT was taken from Ref. [7] and is shown in Fig. 1. The crystallographic data for the unit cell at 100 K is as follows: Space group $P2_1/c$, $a=9.3129$ Å, $b=5.4458$ Å, $c=9.0261$ Å, $\beta=101.464°$, $Z=4$. A periodic lattice geometry optimization and vibrational analysis was performed with the DMol3 [38] package on the SGI Origin Array located at the Aeronautical Systems Major Shared Resource Center. The BLYP [38] functional was used for all DMol3 calculations in conjunction with a dnd numerical basis set. 'Fine' grid spacing was employed in all calculations.

Inelastic neutron scattering spectra (including overtones, combinations and phonon wings) were calculated from the BLYP/dnd normal mode eigenvectors using the A-Climax program v.5.1.3 [39]. In this program, the normal vibrational coordinates are mass-weighted and the scattering cross sections of the different atoms are taken into account. A Debye–Waller factor is accounted for in all fundamentals, overtone, and combination vibrations, which attenuates the vibrational intensities at higher frequencies. Overtone and combination intensities are calculated with their frequencies being assumed as the sum of the component fundamentals.

3. Results

3.1. Geometry

The β-NTO geometry optimized at the BLYP/dnd level is presented in Table 1. The numbering in Table 1 is consistent with the numbering scheme employed in Fig. 1a. The corresponding experimental X-ray diffraction values of β-NTO are shown at both 100 and 273 K. Previously published geometric parameters of a generic isolated NTO molecule are presented at the MP2/6-311G**, B3LYP/6-311G** and B3LYP/6-311++G** theory levels. It is interesting to note that all methods produce a very similar geometry. The BLYP/dnd bond lengths differ from the crystal averages with rms deviations of 0.017 Å (298 K) and 0.014 Å (100 K). The rms deviations in the MP2/6-311G** bond lengths are 0.018 Å (298 K) and 0.017 Å (100 K). In the isolated molecule B3LYP/6-311G** results, the rms deviations increase to 0.019 Å at both 298 and 100 K. The corresponding values for the larger basis set B3LYP/6-311++G** calculation are 0.018 Å (298 K) and 0.019 Å (100 K). The largest deviations between the BLYP/dnd and generic isolated molecule calculated structures are observed primarily between the bond lengths of atoms involved in the hydrogen-bonding network, such as N9–O11 and C3–O7. We believe that the inclusion of the effect of hydrogen bonding on the structure of the molecules in the solid is an

Table 1
Bond lengths (Å) and angles (°) for β-NTO

	BLYP/dnd	MP2 6-311G**[a]	B3LYP 6-311G**[a]	B3LYP 6-311++G**[a]	Exp[b] (298 K)	Exp[b] (100 K)
N1–N2	1.360	1.362	1.359	1.358	1.366	1.370
N2–C3	1.390	1.394	1.398	1.398	1.369	1.368
C3–N4	1.388	1.407	1.405	1.403	1.373	1.377
N4–C5	1.361	1.358	1.365	1.366	1.352	1.352
C5–N1	1.311	1.306	1.290	1.291	1.290	1.295
N2–H6	1.035	1.009	1.008	1.009		
C3–O7	1.235	1.209	1.203	1.205	1.228	1.235
N4–H8	1.050	1.009	1.008	1.009		
C5–N9	1.438	1.448	1.451	1.452	1.444	1.444
N9–O10	1.247	1.224	1.214	1.215	1.226	1.230
N9–O11	1.243	1.234	1.230	1.230	1.212	1.222
N1–N2–C3	112.900	115.480	114.570	114.470	113.000	112.900
N2–C3–N4	103.200	100.270	100.540	100.700	103.500	104.000
C5–N1–N2	103.500	102.160	103.290	103.380	102.600	102.300
H6–N2–N1	119.000	119.550	120.090	120.060		
O7–C3–N2	130.000	130.060	129.630	129.490	127.000	126.900
O7–C3–N4	126.800	129.670	129.840	129.810	129.500	129.100
H8–N4–C3	125.500	125.700	126.080	125.930		
N9–C5–N4	124.000	121.590	121.740	121.880	123.100	123.000
O10–N9–C5	117.500	117.880	118.270	118.460	117.200	117.100
O11–N9–C5	116.500	114.910	114.670	114.730	117.100	116.700
O10–N9–O11	126.100	127.210	127.050	126.800	125.700	126.200

[a] Values are as reported in Ref. [4].
[b] Reported in Ref. [7].

important aspect of a proper description of the vibrations of these species.

There is some evidence of electron rearrangement in the BLYP/dnd bond lengths, presumably due to hydrogen bonding in the solid-state. The C=O bond is 0.03 Å longer in the solid-state calculations than in the isolated molecule. The BLYP/dnd calculated bond length is in close agreement with the X-ray diffraction results at 100 K [7]. Another possible indication of electron rearrangement is revealed in the calculated bond length of N4–H8. This bond lengthens from 1.009 Å in the isolated molecule MP2/6-311G** calculations to 1.050 Å in the BLYP/dnd solid-state calculations. Unfortunately, we are unable to confirm this experimentally. The N4–H8 distance was not reported in the most recent structural analysis of β-NTO [7] and the positions of the hydrogen atoms were not precisely determined in the 1993 X-ray structural determination by Lee et al. [9]. A neutron diffraction study is currently underway in our laboratory, but will be discussed elsewhere [40].

3.2. Molecular vibrations

The experimental INS spectra and BLYP/dnd theoretical spectrum are shown in Fig. 2. Table 2 presents the mode assignments and fundamental vibrational frequencies of β-NTO. Our mode assignments are in close agreement with those given by Sorescu et al. [4]; however, our assignments reveal the contribution of the hydrogen bonding. The INS frequencies are compared to the BLYP/dnd calculated frequencies, the previously published isolated molecule calculated frequencies, and the IR frequencies of α-NTO. There is good agreement between the BLYP/dnd calculated INS frequencies and the experimental INS frequencies. A comparison of the INS vibrational frequencies of β-NTO to the IR vibrational frequencies reported by Sorescu et al., which were thought to be from α-NTO, indicates significant differences between the vibrational frequencies of the two polymorphs. IR and Raman frequencies of β-NTO are not available at this time, but we hope our report stimulates interest in obtaining them.

The vibrational signals between ~10 and 1400 cm^{-1} can be compared with experiment on the basis of the BLYP/dnd calculated frequencies and intensities. As shown in Fig. 2, the INS and BLYP/dnd calculations are in good agreement with one another, and both the peak spacings and relative intensities are reproduced. In general, the BLYP/dnd calculations slightly overestimate the vibrational frequencies, a typical result of DFT. The BLYP/dnd calculation quantitatively gives the correct intensities to 1400 cm^{-1}. The rms deviation between experimental and the BLYP/dnd results is 8.43 cm^{-1}. The corresponding rms values for the isolated molecule calculations are, at 58.45 cm^{-1} (MP2/6-311G**), 61.88 cm^{-1} (B3LYP/6-311G**) and 61.09 cm^{-1} (B3LYP/6-311++G**), notably larger than the solid-state BLYP/dnd rms value. The large rms deviations of the isolated molecule calculations reflect the large effect hydrogen bonding has on the vibrational frequencies and indicate the necessity of including these interactions in a quantum chemical calculation.

The experimental INS spectrum in Fig. 2 shows a rather large background contribution from ~530 to 1400 cm^{-1}. It is observed that, while the BLYP/dnd calculations indicate some contribution to the background from a phonon wing, this does not completely account for the large background present. We believe that there was a small fraction of water in the sample, which gives rise to the additional background contribution in this spectral region. This could be confirmed by the appearance of an O–H band between 3200 and

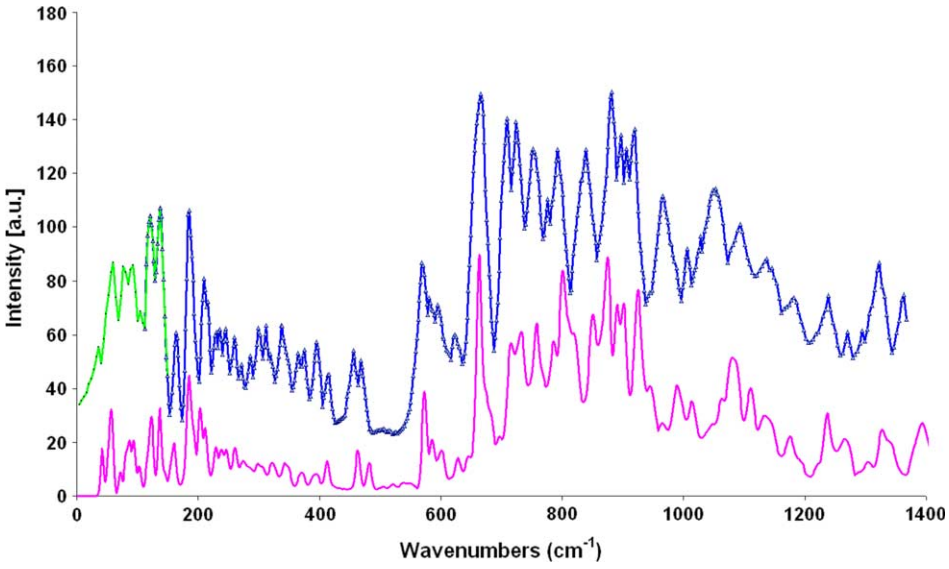

Fig. 2. The β-NTO INS spectra to 1400 cm^{-1} using the TOF instrument (circles) and FANS instrument (triangles). The A-Climax BLYP/dnd simulated INS spectrum is shown as a solid line. The experimental spectra have been scaled for clarity.

Table 2
Fundamental INS and calculated vibrational frequencies of β-NTO (cm^{-1})

	INS		BLYP/dnd		MP2/6-311G**	B3LYP/6-311G**[a]	B3LYP/6311++G**[a]	Matrix IRa	Thin-film IRa	Assignment
	Frequency	Intensity	Frequency	Intensity						
1	77	20	83	20	69	78	77	No	No	N–N skeletal deformation
2	137	52	137	35	132	138	135	No	No	C–N–H bend, N–H wag OP
3	165	31	171	20	192	195	194	No	No	Skeletal deformation IP, NO_2 IP wag
4	186	70	186	51	258	292	288	No	No	Skeletal deformation OP, NO_2 OP bend
5	210	46	214	33	390	390	389	No	No	C–N deformation, N–O wag IP
6	339	28	349	15	414	449	447	No	No	N–H bend OP
7	458	19	465	14	444	468	470	No	No	C–N deformation, N–O wag, N–H def IP
8	468	16	484	12	500	523	517	512	480	N–H bend OP
9	571	50	573	39	553	562	561	573	606	C–N deformation IP, N–C=O deformation, N–H bend
10	662	105	664	90	604	628	625	613	693	N–H bend OP, C–N OP ring deformation
11	710	99	717	75	682	717	708	730	728	N–H bend OP, C–N OP ring deformation
12	724	89	734	72	710	727	725	No	No	N–H deformation, N–N stretch
13	754	78	759	64	715	737	727	738	751	N—H bend OP, NO_2 bend OP
14	789	75	802	73	797	813	810	822	805	N–H wag, N–O scissor
15	881	103	891	89	947	944	946	971	830	N–H bend OP
16	1000	49	991	40	962	973	971	991	1021	Skeletal def.
17	1090	60	1083	51	1095	1046	1047	1085	1111	C–N stretch N–H wag OP
18	1238	40	1220	32	1150	1160	1163	1174	1185	C–N stretch N–H wag OP
19	1271	26	1274	22	1216	1218	1219	1257	1282	C–N stretch N–H wag IP
20	1323	51	1330	43	1306	1322	1313	1338	1343	C–N stretch N–H wag IP
21	1395	40	1400	35	1337	1343	1344	1361	1477	N–H deformation
22			1485	40	1437	1415	1411	1463	1550	N–H deformation, C–N stretch
23			1551	35	1520	1557	1541	1563	1605	C–N stretch, N–H deformation
24			1688	24	1723	1584	1570	1768	1695	N–H bend, C–N stretch
25			1727	17	1794	1801	1779	1789	1716	C=O stretch
26			3235	32	3510	3525	3518	3489	3200	N–H stretch
27			3266	35	3514	3527	3519	No	No	N–H strech

A 'No' refers to a frequency that was not reported. The Matrix IR and Thin-film IR were reported to belong to α-NTO. Intensities are reported in arbitrary units to facilitate comparison.

[a] Values are as reported in Ref. [4].

3600 cm^{-1}, but unfortunately our instrument cannot access this region.

There are six fundamental vibrational modes, namely ν_6, ν_8, ν_{12}, ν_{14}, ν_{15}, and ν_{18}, where frequency deviations of 10 cm^{-1} or greater are observed between the experimental INS and BLYP/dnd frequencies. As can be seen from Table 2, these modes primarily involve large out-of-plane hydrogen atom motion. Based on the crystalline geometry shown in Fig. 1b, these deviations suggest that the hydrogen bond network is not modeled exactly in our solid-state calculations and that the hydrogen bonds are calculated to be longer than the corresponding crystallographic bond lengths. The solid-state calculations, however, represent a substantial improvement over the isolated molecule calculations, which have frequency deviations as large as 55 cm^{-1} for these particular modes, even after scaling by the accepted scaling factor [41].

3.3. Phonon modes

The frequencies and assignments of the β-NTO phonons are provided in Table 3. Four well-defined peaks in the TOF β-NTO spectrum appear with maxima at (P_1) 37 cm^{-1}, (P_2) 60 cm^{-1}, (P_3) 93 cm^{-1}, and (P_4) 235 cm^{-1}. Fig. 2 shows

Table 3
Phonon and combination band assignments for β-NTO

	INS		BLYP/dnd	
	Frequency	Intensity	Frequency	Intensity
P_1	37	25	42	18
P_2	60	49	57	36
P_3	93	55	94	39
P_4	235	27	241	18
Combinations				
P_1+P_2	105	29	105	20
P_1+P_3	121	58	124	35
P_2+P_3	230	32	231	25
$P_2+\nu_4$	246	27	248	16
P_1+P_4	272	19	278	13
$P_4+\nu_1$	313	33	308	25
$P_1+\nu_6$	375	24	373	18
$P_2+\nu_{11}$	776	78	787	65

All values are reported in cm^{-1}. Intensities are reported in arbitrary units to facilitate comparison.

that the BLYP/dnd calculations have good agreement with the experimental results in terms of both frequency and the general pattern of intensity.

The phonon overtone and combination bands observed in the INS spectrum of β-NTO are summarized in Table 3. There are four phonon combination bands which are assigned to P_1+P_2 (105 cm^{-1}), P_1+P_3 (121 cm^{-1}), P_2+P_3 (230 cm^{-1}) and P_1+P_4 (272 cm^{-1}). Four instances of coupling between the phonon modes and the fundamental vibrations are found in the INS spectrum, which are assigned to $P_2+\nu_4$ (246 cm^{-1}), $P_4+\nu_1$ (313 cm^{-1}), $P_1+\nu_6$ (375 cm^{-1}) and $P_2+\nu_{11}$ (776 cm^{-1}). Although combination modes occur between all vibrational modes with a resulting intensity largely dependent on the intensity of the fundamental vibrations, it is interesting to note that the four most intense combination modes that are discussed above all contain a significant degree of N–H vibration. This suggests that these four modes may be considered as 'doorway modes' and offers a possible mechanism for bond breaking, which is induced by phonon excitation. Furthermore, an intense combination of a phonon band and fundamental vibration at 776 cm^{-1} suggests that vibrations up to 800 cm^{-1} or higher may also play a role in vibrational up-pumping.

3.4. Combinations and overtones

The overtone and combination bands of the fundamental vibrations observed in the INS spectra of β-NTO are summarized in Table 4. Combination and overtone vibrations typically display more anharmonic character than fundamental transitions because they have much stronger interactions. Therefore, the accurate representation

Table 4
The overtone and combination bands of the fundamental vibrations

	INS		BLYP/dnd		MP2/6-311G**[a]	B3LYP/ 6-311G**[a]	B3LYP/ 6-311++G**[a]
	Frequency	Intensity	Frequency	Intensity			
$\nu_1+\nu_2$	216	40	210	27	201	216	212
$\nu_4+\nu_1$	262	29	275	20	327	370	365
$\nu_1+\nu_5$	288	22	295	15	459	468	466
$\nu_2+\nu_3$	300	30	302	22	324	333	329
$\nu_2+\nu_4$	321	23	330	15	390	430	423
$2\times\nu_4$	367	25	378	19	516	584	576
$\nu_5+\nu_4$	395	27	405	15	648	682	677
$\nu_6+\nu_1$	415	25	427	15	483	527	524
$\nu_7+\nu_2$	597	47	597	31	576	606	605
$\nu_7+\nu_3$	625	29	630	19	636	663	664
$\nu_{11}+\nu_2$	842	87	855	73	814	855	843
$\nu_{11}+\nu_4$	897	93	888	71	940	1009	996
$\nu_{12}+\nu_4$	905	87	897	71	968	1019	1013
$\nu_{11}+\nu_5$	920	100	926	83	1072	1107	1097
$\nu_{13}+\nu_4$	946	50	950	43	973	1029	1015
$\nu_{13}+\nu_5$	968	65	966	50	1105	1127	1116
$\nu_{15}+\nu_2$	1015	56	1016	39	1079	1082	1081
$\nu_{11}+\nu_6$	1053	92	1047	70	1096	1166	1155
$\nu_{15}+\nu_4$	1068	75	1064	61	1205	1236	1234
$\nu_7+\nu_{10}$	1112	40	1112	37	1048	1096	1095
$\nu_{16}+\nu_2$	1138	44	1138	39	1094	1111	1106
$\nu_{11}+\nu_8$	1177	37	1179	21	1182	1240	1225
$\nu_{13}+\nu_7$	1202	45	1202	37	1159	1205	1197
$\nu_{14}+\nu_8$	1268	41	1266	33	1297	1336	1327
$\nu_{17}+\nu_5$	1306	21	1308	15	1485	1436	1436

All values are reported in cm^{-1}. Intensities are reported in arbitrary units to facilitate comparison.
[a] Values are as reported in Ref. [4].

of these transitions is an important challenge for the harmonic approximation.

One overtone transition ($2\nu_4$) is observed in the INS spectrum at 367 cm^{-1}. The BLYP/dnd frequency calculated with the A-Climax program deviates by 11 cm^{-1} from the experimental value. This deviation presumably reflects some degree of anharmoncity. The notable intensity difference between the calculated and experimental spectra can be justified by noting the slight difference in intensity between the calculated and experimental fundamental vibration, ν_4.

In many cases, the calculated vibrational frequencies of the combination transitions are adequately described with the BLYP/dnd calculations. The largest frequency deviations are observed for combination modes that have a significant contribution from hydrogen motion, primarily ν_1, ν_4, ν_6, and ν_{11}. This is consistent with the X-ray diffraction, which indicates the anharmonic nature of the hydrogen bonds of β-NTO. The isolated molecule frequencies deviate significantly, often up to 200 cm^{-1}, from the INS experimental frequencies for combinations of these fundamental vibrations. The anharmonic nature of β-NTO is also reflected in the inaccurate calculated intensities of several combination bands.

4. Conclusions

The vibrational spectrum of the energetic material β-NTO was calculated using the BLYP/dnd full periodic representation employed in DMol3 and compared to the INS experimental frequencies. The simulated INS spectrum was constructed using the A-Climax program and included combinations and overtones up to four quanta. The degree of agreement between the theoretical and experimental vibrational spectra demonstrates the advantages of the A-Climax program as a useful method for calculations and analysis of the vibrational spectroscopy of polyatomic molecules.

Our analysis of the INS vibrational spectra verifies that the molecular packing of NTO in its crystalline lattice plays an important role in the general pattern of the vibrational spectrum of the molecule. By comparing the similarities between calculated and measured INS spectral plots, we attempted to establish a one-to-one correspondence between calculated and measured bands, thereby assigning the normal modes. In addition, four phonon modes were assigned. Four instances of intense vibrational coupling between the phonon and internal modes were found. All internal modes that were coupled to the phonon modes were found to have significant N–H character, suggesting a possible mechanism for bond breaking induced by excitation of phonons. Evidence was found of coupling between the phonon and fundamental vibrations up to 776 cm^{-1}, indicating higher frequency modes might also play a role in vibrational up-pumping.

We found generally good agreement between the calculated geometry of the NTO molecule and the experimentally determined geometry of the β-NTO molecule at 100 K. We also found good agreement between both the intensities and frequencies of the solid-state BLYP/dnd calculations and the experimental INS values. In general, this work indicates that the quantum chemical description of highly hydrogen-bonded systems requires a proper treatment of the number of degrees of freedom of the lattice, the effects of intermolecular interactions on the structure of the molecule and the effect of intermolecular interactions on the coupling of vibrations of the molecules in the lattice.

Acknowledgements

The NIST Center for Neutron Research is acknowledged for providing neutron beam access on the FANS and TOF instruments. The Wright-Patterson Aeronautical Major Shared Resource Center is thanked for access to the DMol3 program. Picatinny Arsenal is thanked for providing the sample of β-NTO. An NRC Fellowship with the Army Research Laboratory supported J.C. during the course of this research.

References

[1] K.-Y. Lee, M.D. Coburn, US Patent 4733610 (1988).
[2] K.-Y. Lee, R. Gilardi, Struct. Prop. Energet. Mat. 296 (1993) 237.
[3] Y.-M. Wang, C. Chen, S.-T. Lin, J. Mol. Struct. Theochem 460 (1999) 79.
[4] D.C. Sorescu, T.R.L. Sutton, D.L. Thompson, D. Beardall, C.A. Wright, J. Mol. Struct. 384 (1996) 87.
[5] B.M. Dobratz, The Insensitive High Explosive TATB: Development and Characterization-1888 to 1994, Los Alamos National Lab, Los Alamos, NM, 1995.
[6] R.D. Gilardi, R.J. Butcher, Acta Cryst. E57 (2001) o738.
[7] N.B. Bolotina, E.A. Zhurova, A.A. Pinkerton, J. Appl. Cryst. 36 (2003) 280.
[8] D.C. Sorescu, D.L. Thompson, J. Phys. Chem. B 101 (1997) 3605.
[9] K.-Y. Lee, R. Gilardi, Structure and properties of energetic materials in: D.H. Lienbenbur, R.W. Armstrong, J.J. Gilman (Eds.), Materials Research Society vol. 296 (1993), p. 237.
[10] H.V. Brand, R.L. Rabie, D.J. Funk, I. Diaz-Acosta, P. Pulay, T.K. Lippert, J. Phys. Chem. B 106 (2002) 10594.
[11] S.D. McGrane, A.P. Shreve, J. Chem. Phys. 119 (2003) 5834.
[12] Y.A. Gruzdkov, Y.M. Gupta, J. Phys. Chem. A 105 (2001) 6197.
[13] N.F. Fell, J.M. Widder, S.V. Medlin, J.B. Morris, R.A. Pesce-Rodriguez, K.L. McNesby, J. Raman Spect. 27 (1996) 97.
[14] J.A. Ciezak, S.F. Trevino, Chem. Phys. Lett. 403 (2005) 329.
[15] J.A. Ciezak, S.F. Trevino, J. Mol. Struct. Theochem 723 (2005) 241.
[16] B.S. Jursic, J. Mol. Struct. Theochem 530 (2000) 21.
[17] D.S. Moore, S.D. McGrane, J. Mol. Struct. 661 (2003) 561.
[18] C. Aubauer, K. Karaghiosoff, T.M. Klapotke, G. Kramer, A. Schulz, J. Weigand, Z. Anorg. Allg. Chem. 627 (2001) 2547.
[19] A. Hammerl, T.M. Klapotke, H. Noth, M. Warchhold, G. Holl, M. Kaiser, U. Ticmanis, Inorg. Chem. 40 (2001) 3570.
[20] A. Hammerl, G. Holl, M. Kaiser, T.M. Klapotke, H. Piotrowski, Z. Anorg. Allg. Chem. 629 (2003) 2117.

[21] D.D. Dlott, M.D. Fayer, J. Chem. Phys. 92 (1990) 3798.
[22] S. Chen, W.A. Tolbert, D.D. Dlott, J. Phys. Chem. 98 (1994) 7759.
[23] A. Tokamakoff, M.D. Fayer, D.D. Dlott, J. Phys. Chem. 97 (1993) 1901.
[24] L.E. Fried, A.J. Ruggiero, J. Phys. Chem. 98 (1994) 9786.
[25] B.S. Hudson, J. Phys. Chem. A 105 (2001) 3949.
[26] G.J. Kearley, M.R. Johnson, M. Plazanet, E. Suard, J. Chem. Phys. 115 (2001) 2614.
[27] M. Plazanet, N. Fukushima, M.R. Johnson, Chem. Phys. 280 (2002) 53.
[28] M.R. Johnson, K. Parlinski, I. Natkaniec, B.S. Hudson, Chem. Phys. 291 (2003) 53.
[29] A. Pawlukojc, I. Natkaniec, G. Bator, E. Grech, L. Sobczyk, Spect. Chem. Acta A60 (2004) 2875.
[30] B.S. Hudson, D.G. Allis, S.F. Parker, A.J. Ramirez-Cuesta, H. Herman, H. Prinzbach, J. Phys. Chem. A109 (2005) 3418.
[31] M. Plazanet, F. Fontain-Vive, K.H. Gardner, V.T. Forsyth, A. Ivanov, A.J. Ramirez-Cuesta, M.R. Johnson, J. Am. Chem. Soc. 127 (2005) 6672.
[32] D.G. Allis, B.S. Hudson, Chem. Phys. Lett. 385 (2004) 166.
[33] Certain commercial software and instruments are identified in this paper to foster understanding. Such identification does not imply recommendation or endorsement by the National Institute of Standards and Technology, nor does it imply that the software or equipment identified are necessarily the best available for this purpose.
[34] J.R.D. Copley, D.A. Neumann, W.A. Kamitakahara, Can J. Phys. 73 (1995) 763.
[35] T.J. Udovic, D.A. Neumann, J. Leão, C.M. Brown, Nucl. Instrum. Methods Phys. Res. 517 (2004) 189.
[36] www.ncnr.nist.gov/instruments/fcs.
[37] http://www.ncnr.nist.gov/dave.
[38] B. Delley, J. Chem. Phys. 92 (1990) 508.
[39] A.J. Ramirez-Cuesta, Comp. Phys. Comm. 157 (2004) 226.
[40] J.A. Ciezak, S.F. Trevino, unpublished results.
[41] A.P. Scott, L. Radom, J. Phys. Chem. 100 (1996) 16502.